Coalescence Collision of Two Droplets: Bubble Entrapment and the Effects of Important Parameters

Mohammad Passandideh-Fard[1], Ehsan Roohi[2]
Mechanical Engineering Department, Ferdowsi University of Mashhad
Mashhad, Iran
mpfard@um.ac.ir

Abstract

In this study, coalescence collision of two water droplets is studied using a modified Volume of Fluid (VOF) method. The focus of this work is on head-on binary collision of two droplets; the effects of Reynolds number, drop size ratio and impact velocity on the coalescence process are investigated. In addition, air bubble entrapment phenomenon during droplet collision is discussed.

Keywords: Spray, Atomization, Coalescence Collision, Droplet Impact, Air Bubble Entrapment, Volume of Fluid, Free Surface Flow, Numerical Simulation

Introduction

Coalescence collision, the phenomenon in which two liquid droplets combine and generate one single drop via a collision (Fig. 1), is an essential feature of many industrial and natural processes. This phenomenon, therefore, has been the subject of numerous studies. Spray coating, liquid spraying, internal combustion engine sprays, atmospheric raindrop formations and icing, surface treatment and liquid-liquid extraction are only a few of the more common examples. In diesel engine sprays, for example, coalescence affects the drop size in the engine cylinder, which could affect combustion characteristics. Coalescence of liquid drops plays a fundamental role in meteorological studies of precipitation formation. Also, success of liquid-liquid extraction operations depends on subsequent coalescence [1].

Typically, collision outcome can be categorized by Weber number, Reynolds number and impact parameter (I),

$$\mathrm{Re} = \frac{\rho_l V_{rel} D_s}{\mu}, We = \frac{\rho_l V_{rel}^2 D_s}{\sigma}, I = \frac{2b}{D_s + D_b}. \qquad (1)$$

where σ and μ denote liquid surface tension and viscosity. V_{rel} is the droplet relative velocity, and D_s and D_b are diameters of smaller droplet and bigger droplet, respectively. The impact parameter characterizes the eccentricity of the collision and *b* is defined as the distance from the center of one droplet to the relative velocity vector placed on the center of the other droplet. It has been reported in the literature [2] that five main collision regimes may exist as illustrated by five different regions in Fig. 2 [(a) to (e)]:

- Permanent coalescence after minor deformation (stable coalescence) (a),
- Bouncing (b),
- Permanent coalescence after substantial deformation (c),
- Temporal coalescence followed by separation for near head-on collision (reflexive separation) (d),
- Temporal coalescence followed by separation for off-center collisions (stretching separation) (e)

Regime (a) occurs when the droplet kinetic energy is smaller than its surface energy. In

1- Assistant Professor
2- Graduate Student

regime (b), the droplet energy is not enough to push out the gas film enclosed between droplet interfaces. The two droplets in this case are separated by a very thin gas film which prevents coalescence and, therefore, bouncing occurs. This regime is observed in hydrocarbon droplets [3] but for water droplets it may occur when the gas density is higher than that of the usual ambient, as stated by Qian and Law [4]. In regime (c), the droplet energy is sufficient to push out the gas film and coalescence could occur. For higher droplet's kinetic energy, regime (d) is observed. After many oscillations, breakup occurs and satellite droplets appear. Regime (e) occurs for off-center collision with high impact parameters. In this regime, breakup mechanism mainly refers to shear forces instead of oscillation forces. A critical Weber number, We_c, defines the boundary between these regimes. Ashgriz and Poo [5] experimentally investigated water droplet collisions for Weber numbers less than 100, and size ratios ($\Delta=D_s/D_b$) of 0.5, 0.75 and 1. They found a critical Weber number between coalescence and reflexive separation equal to 19 for head-on collisions of water droplets. This limit depends on both the liquid and ambient gas pressure [4].

Due to its wide applications, droplet collision has been the subject of many numerical studies. Melean and Sigalotti [1] presented a numerical calculation of head-on and off-center binary collision of van der Waals liquid drops using the method of smoothed particle hydrodynamics (SPH). Tanguy and Berlemont [2] used level set method to simulate droplet collision at different collision regimes for water and hydrocarbon liquids. Nobari et al. [6] used a front tracking method to study the boundary between the coalescence and bouncing in head-on drop collision. Mashayek et al. [7] investigated the role of viscosity, droplet impact velocity, size ratio and internal circulation on the coalescence process, using a Galerkin finite element method.

In this study, 2D/axisymmetric simulations of binary droplet collisions are performed using a modified "Volume of Fluid" (VOF) method and Youngs' algorithm [8]. The main focus is on head-on coalescence collision.

Numerical Method

The numerical method is based on an improved version of RIPPLE computer code [9]. These improvements have been described in detail by Bussmann et al. [10].

The governing equations are

$$\begin{aligned} &\vec{\nabla}.\vec{V} = 0 \\ &\frac{\partial\left(r\vec{V}\right)}{\partial t} + \vec{\nabla}.\left(r\vec{V}\vec{V}\right) = -\vec{\nabla}P + \vec{\nabla}.\left(\vec{t}\right) + F_b \end{aligned} \tag{2}$$

where $\vec{V}$ is the velocity vector, P is the pressure and F_b represents all body forces acting on the fluid.

The continuum surface force (CSF) method [11] was used to model surface tension as a body force that acts only on interfacial cells. The free surface of the droplet is reconstructed using VOF model by means of a scalar field $f(x,t)$, where,

$$f(x,t) = \begin{cases} 1 & \text{in liquid} \\ >0,\ <1 & \text{at the liquid-gas interface} \\ 0 & \text{in gas} \end{cases} \tag{3}$$

For incompressible flow, the f function must be regarded as the normalization $f(x,t)=\rho(x,t)/\rho_f$, where ρ_f is the constant fluid density. The discontinuity in f is a Lagrangian invariant, propagating according to

$$\frac{Df}{Dt} = \frac{\partial f}{\partial t} + \vec{V}.\vec{\nabla}f = 0 \tag{4}$$

The above equation is used to track the location of the interface and it is solved according to Youngs' algorithm [8]. Assuming the initial distribution of f to be given, velocity and pressure are calculated after each time step by the following procedure. The f advection begins by defining an intermediate value of f,

$$f^{\%} = f^{n} - dt\,\vec{\nabla}.\left(\vec{V}f^{n}\right) \tag{5}$$

and it could be completed with a "divergence correction,"

$$f^{n+1} = f^{\%} + dt\left(\vec{\nabla}.\vec{V}\right)f^{n} \tag{6}$$

New velocity field is calculated according to the projection method. First, an intermediate velocity is obtained,

$$\frac{\vec{V}^{\%} - \vec{V}^{n}}{dt} = -\vec{\nabla}.\left(\vec{V}\vec{V}\right)^{n} + \frac{1}{r^{n}}\vec{\nabla}.\vec{t}_{n} + \frac{1}{r^{n}}F_b^{n} \tag{7}$$

Pressure Poisson equation is then solved to obtain the pressure field,

$$\vec{\nabla}.\left(\frac{1}{r^{n}}\vec{\nabla}P^{n+1}\right) = \frac{1}{\Delta t}\vec{\nabla}.\vec{V}^{\%} \tag{8}$$

Next, new time velocity filed is calculated by considering the pressure field implicitly,

$$\frac{\vec{V}^{n+1} - \vec{V}^{\%}}{\Delta t} = -\frac{1}{r^{n}}\vec{\nabla}.P^{n+1} \tag{9}$$

The reader is referred to *Ref.* [10] for further details of the numerical method.

Model Validation

The 2D/axisymmetric solution domain, 1.2 mm in radius and 3.36 mm in axial direction, subdivided into a structured uniform mesh with a 90×252 grid points. The grid size was selected on the basis of a mesh refinement study where four different mesh sizes with 30×84, 60×168, 90×252 and 120×336 grid points (corresponding to a resolution of $\Delta x=\Delta y=40$ μm, $\Delta x=\Delta y=20$ μm, $\Delta x=\Delta y=13.3$ μm, and $\Delta x=\Delta y=10$ μm, respectively) were examined. In the numerical study of droplet collision, it is common to compare mesh sizes using a geometrical parameter CPR defined as the number of cells per droplet radius. The corresponding values of CPR for the above mesh sizes are 10, 20, 30 and 40, respectively.

To validate the numerical procedure, the first simulation is presented for water droplets 400 μm in radius with a Weber number of 23, an impact parameter of zero, and a droplet relative velocity of 1.44 m/s. This collision case was experimentally studied by Ashgriz and Poo [5] and is shown in Fig. 3a. To simulate this case numerically, we performed a mesh refinement study with four different mesh sizes for which the CPR value ranged from 10 to 40 as explained above. The results are shown in Fig. 3 (b-e). As observed in Fig. 3, increasing the mesh sizes translates in a better comparison between numerical results and experimental photographs. For a value of CPR equal to 30, shown in Fig. 3d where two droplets separated horizontally at time 1.03 ms, we have the best agreement between photographs and numerical images. It should be mentioned that increasing the mesh size beyond a CPR of 30 results in a less accurate solution compared to experiments as seen in Fig. 3e for a CPR of 40. This means that in refining a mesh for the simulation we have a certain limit beyond which the induced numerical errors are increased and the results will no longer improve. This point becomes particularly important when there is breakup during liquid deformation. As a result of this mesh refinement study, a grid size corresponding to CPR=30 was selected for all calculations in this paper.

Results and Discussion

The main focus of this study is on coalescence collision of droplets; therefore, the low Weber number regime is of our interest. Since head-on collision is studied, the impact parameter (I) would typically be zero. The effects of Reynolds number and droplet size ratio are investigated; and the air bubble entrapment phenomenon between colliding droplets is discussed.

Effect of Reynolds Number

In this section, the effects of Reynolds number on coalescence behavior of two equal-sized droplets are studied. Referring to Fig 2, this study considers collisions in region (c) or coalescence after major deformations. Water droplets (density 10^3 kg/m^3, kinematic viscosity 10^{-6}, surface tension 0.072 N/m) 400 μm in radius were tested. Reynolds number was varied by changing impact velocity; Re=240 refers to a relative velocity of 0.30 m/s and Re= 480 refers to 0.60 m/s. Due to the geometrical symmetry, only one slice of the droplets are modeled.

In Fig. 4, the time evolution of droplet deformation for Re=240 and Re=480 is illustrated. Collision dynamics in this collision regime is governed by viscous dissipation. In case (a), images between 0.0 ms and 1.67 ms demonstrate the first half period of coalescence during which the coalesced drop reaches its maximum surface deformation at 1.67 ms. Similarly, images between 0.0 ms and 1.34 ms in case (b) show first half period, but during a shorter time and with a more surface deformation as well as a thinner final state. Along the vertical axis (i.e., axis of symmetry) due to a higher surface energy, internal velocities changes faster. Therefore, there is more viscous dissipation along this axis than along the horizontal direction. The final image of the first half period refers to condition where a concave surface is formed. Therefore, an adverse pressure is generated which prevents further inward movement of the surface [7]. Jiang et al. [3] inferred that about half of the internal kinetic energy is lost during the first half period. In the second row of images in Fig. 4, reverse motion of coalesced droplet toward its maximum height (corresponding to the end of the first oscillation period) is shown. Comparison between the results for the two Reynolds number shows that a higher Reynolds number results in a higher droplet deformation during the period. This fact could also be related to fluid viscosity. Higher Reynolds number refers to lower liquid viscosity if all other parameters (velocity, drop radius) remain constant. As a result, Re number variation demonstrates the

consequences of viscosity changes; i.e. less viscous fluid exhibit higher deformations as there is smaller damping forces. If we define two geometrical parameters, y_{min} and r_{max}, defined as minimum thickness and maximum radius of coalesced droplet, respectively, we will observe that by increasing Re number y_{min} decreases while r_{max} increases. In other words, increasing Re number translates in higher deformations in both axes. The final outcome of collision after oscillations in either of the above cases will be the formation of a spherical coalesced drop.

Air Bubble Entrapment

In coalescence collision, the inertial energy of colliding drops is high enough to push out gas layer entrapped between them. As a result, two drops combine. In lower energy collision, this layer may prevent coalescence and bounce the drops (regime b in Fig. 2). But even in high energy impacts, it is experimentally observed that a small air bubble forms. Mehdi-Nejad et al. [12] reported that air bubble may form under impacting droplet on a solid surface (Fig. 5). Bubble entrapment occurs in the case of droplet impact on a liquid surface as well [13] (e.g., raindrops falling on a poll). Bubble formation may affect physical behaviour considerably. When two drops approach each other, air is forced out in the gap between them. Increased air pressure between drops creates a depression in combined drop in which air is trapped [12]. Air bubble entrapment between colliding drops is clearly visible in Fig. 4 when there is an initial distance between drops. In case of equal droplet collision, air bubble places itself in the middle of coalesced drop and keeps this position during the deformation process. This fact refers to the symmetrical nature (geometry-velocity vector) of the collision. Air bubble is formed in the stagnation point (two droplets' first contact point) where fluid does not move in a symmetrical collision. Air bubble entrapment in unequal drop collision is discussed in the next section.

Effects of Drop Size Ratio and Impact Velocity

Unequal droplet collision simulations, corresponding to drop diameter ratio of 0.5 and for constant relative velocity, are shown in Fig. 6 (a-c). In the first case (Fig. 6a) it is assumed that the upper drop approaches the lower one with a velocity of 0.30 m/s while the lower has no initial velocity. In the second case (Fig. 6b) the two drops have equal velocity of 0.15 m/s, and in the third case (Fig. 6c) the upper one is assumed to be still and the lower moves with a velocity of 0.30 m/s. Reynolds number, based on D_s and V_{rel}, is held constant for all three cases, equal to 120. As observed, there are more deformations in unequal drop collision and more images are required to investigate collision behaviour. In the early stages of collision, the largest deformation occurs near the drops contact point. All three collision cases show similar deformations during collision interval, but with a time delay. As observed, the two ends of the coalesced drop oscillate with a certain phase delay and as this oscillation damps with time, the final state of the coalesced droplet is formed. Case (c) shows the fastest deformation and case (b) exhibits the slowest deformation during collision. This observation means that in unequal collision, the collision dynamics is governed mainly by the bigger droplet. In all three cases, a similar drop is formed after the end of the oscillations.

In the case of unequal drop collision, the position of the entrapped air bubble changes with time and when one droplet has no initial velocity, the bubble is forced out from the coalesced droplet (Fig. 6a and 6c). In Fig. 6a, the air bubble leaves the droplet when the upper droplet gives its energy to lower one, but in Fig. 6c, it exits in the downward motion of the coalesced droplet. As stated, this difference in bubble movement is due to the stagnation point position. In Fig. 6b, the stagnation point undergoes major deformations, but due to equal velocity vector, air bubble remains in the coalesced drop.

Conclusion

In this study, coalescence collision of water droplets was investigated. Different factors affecting the coalescence such as Reynolds number, drop size ratio and impact velocity were discussed. By changing Reynolds number, the effects of viscosity variation could also be investigated. Viscosity acts as a damping force, and oscillation time and amplitude are decreased as viscosity increases. In case of unequal droplet collision, there is higher deformation before reaching the final state. It was shown that an air bubble is formed at the contact point of the two colliding drops. The bubble remained inside the liquid for a symmetrical collision, but forced out in other cases.

References

1- Melean Y., Sigalotti L., "Coalescence of Colliding Van Der Waals Liquid Drops", Int. J. of Heat & Mass Transfer, Vol.48, 2005, pp. 4041-4061.
2- Tanguy S., Berlemont A., "Application of a Level Set Method for Simulation of Droplet Collisions", Int. J. of Multiphase Flow, Vol.31, 2005, pp. 1015-1035.
3- Jiang Y.J., Umemura A., Law C.K., "An Experimental Investigation on the Collision Behavior of Hydrocarbons Droplets", J. Fluid Mech., Vol.234, 1992, pp. 171-190.
4- Qian J., Law C.K., "Regimes of Coalescence and Separation in Droplet Collision", J. Fluid Mech., Vol.331, 1997, pp. 59-80.
5- Ashgriz, N., Poo J., "Coalescence and Separation in Binary Collision of Liquid Drops", J. Fluid Mech., Vol.221, 1990, pp. 183-204.
6- Nobari M., Jan Y.J., Tryggvason G., "Head-on Collision of Dropes-A Numerical Investigation", Phys. Fluid, Vol.8, No.1, 1996, pp. 29-42.
7- Mashayek, F., Ashgriz, N., Minkowycz W.J., Shotorban B., "Coalescence Collision of Liquid Drops", Int. J. of Heat & Mass Transfer, Vol.46, 2003, pp. 77-89.
8- Youngs D.L., "Time dependent multi material flow with large fluid distortion", Num. Methods for Fluid Dynamics, N.Y, 1982, pp. 273-285.
9- Kothe D.B., Mjolsness R.C., Torrey M.D., "RIPPLE: A Computer Program for Incompressible Flows with Free Surfaces", Technical Report LA-12007-MS, LANL (1991).
10- Bussmann M., Mosthghimi J., Chandra S., "On a Three-Dimensional Volume Tracking Model of Droplet Impact", Phys. Fluid, Vol. 11, 1999, p. 1406.
11- Brackbill J.U., Kothe D.B., Zamach C., "A continuum method for modeling surface tension, Comp. Physics", V. 100, 1992, pp. 335-354.
12- Mehdi-Nejad V., Mostaghimi J., Chandra S., "Air Bubble Entrapment under an Impacting Droplet", Phys. of Fluid, Vol. 15, No. 1, 2003, pp. 173-183.
13- Pumphery H.C., Elomore P.A., "The Entrapment of bubbles by drop impacts", J. Fluid Mech., Vol. 220, 1990, p.539.

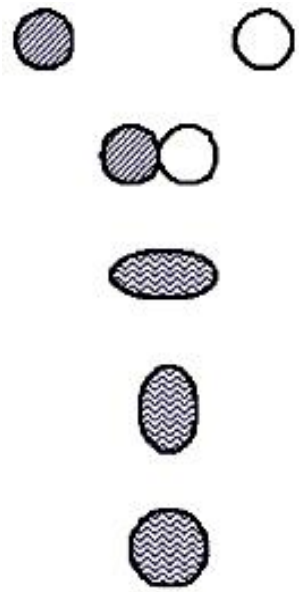

Figure 1: Schematic of coalescence.

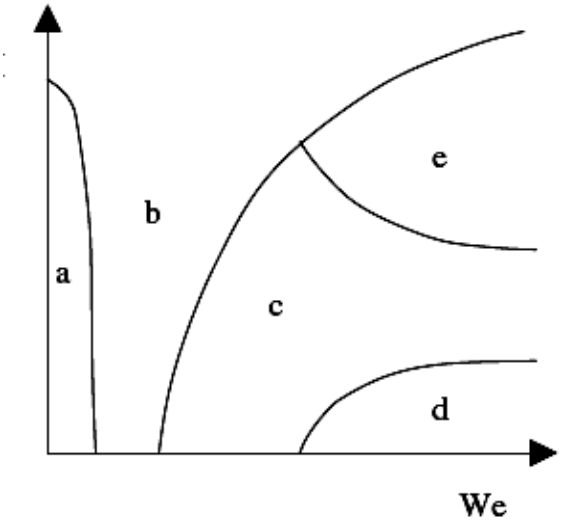

Figure 2: Different droplet collision regimes.

a)

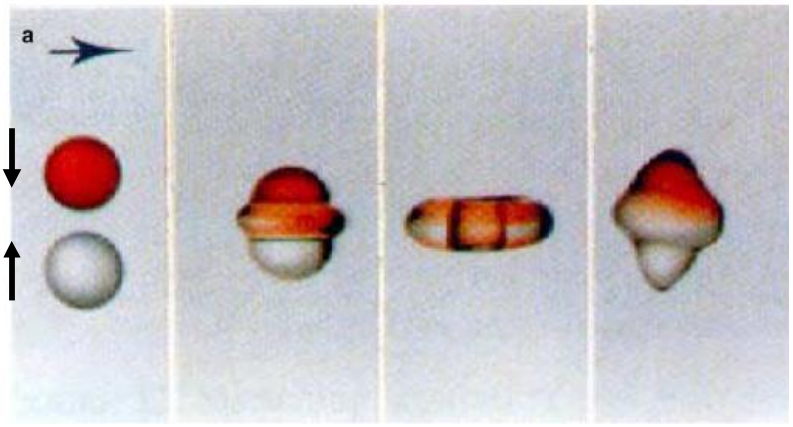

b)

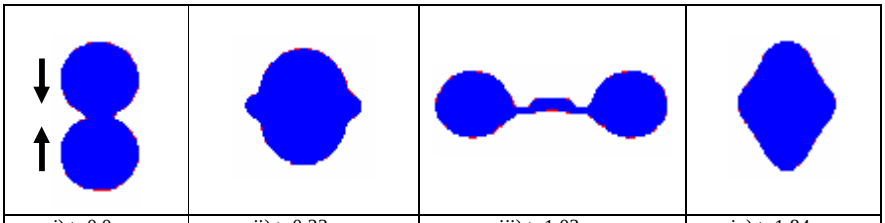

i) t=0.0 ms	ii) t=0.33 ms	iii) t=1.03 ms	iv) t=1.84 ms

c)

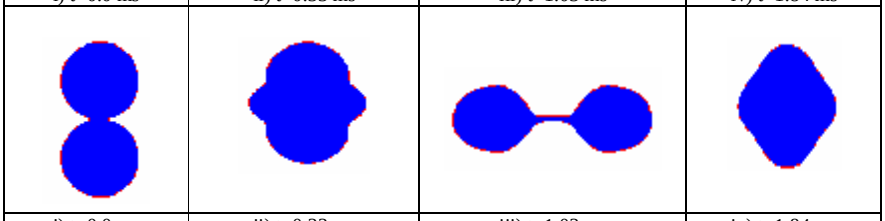

i) t=0.0 ms	ii) t=0.33 ms	iii) t=1.03 ms	iv) t=1.84 ms

d)

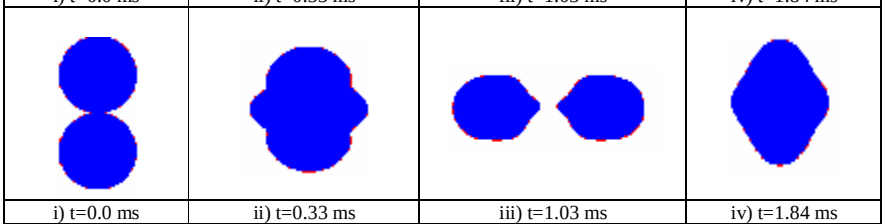

i) t=0.0 ms	ii) t=0.33 ms	iii) t=1.03 ms	iv) t=1.84 ms

e)

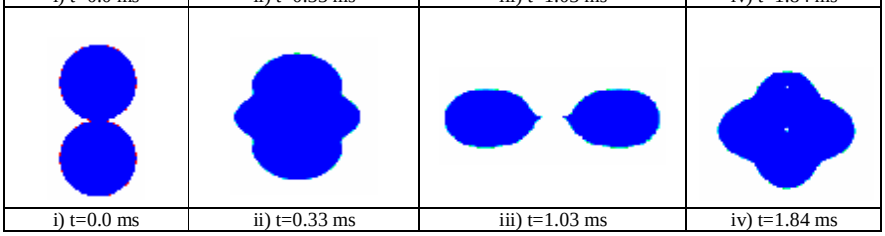

i) t=0.0 ms	ii) t=0.33 ms	iii) t=1.03 ms	iv) t=1.84 ms

Figure 3: Time evolution of droplet deformation and a comparison between a) experimental photographs [5] and the results of numerical simulation with four different mesh sizes of b) CPR=10 , c) CPR=20 , d) CPR=30 and e) CPR=40.

a)

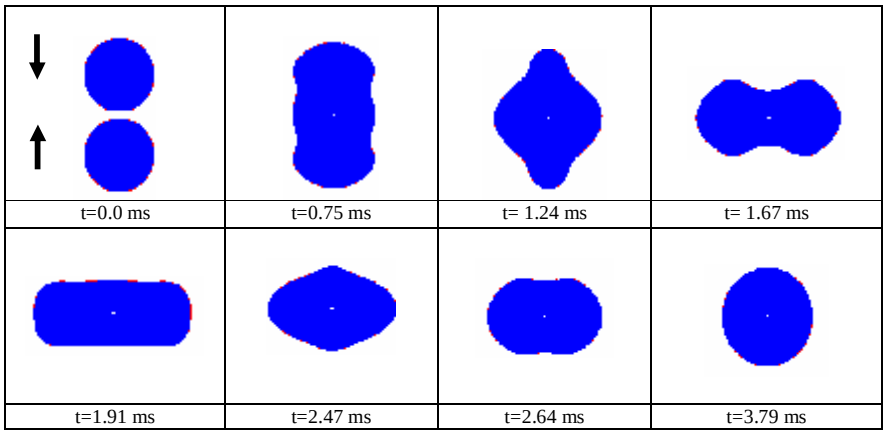

b)

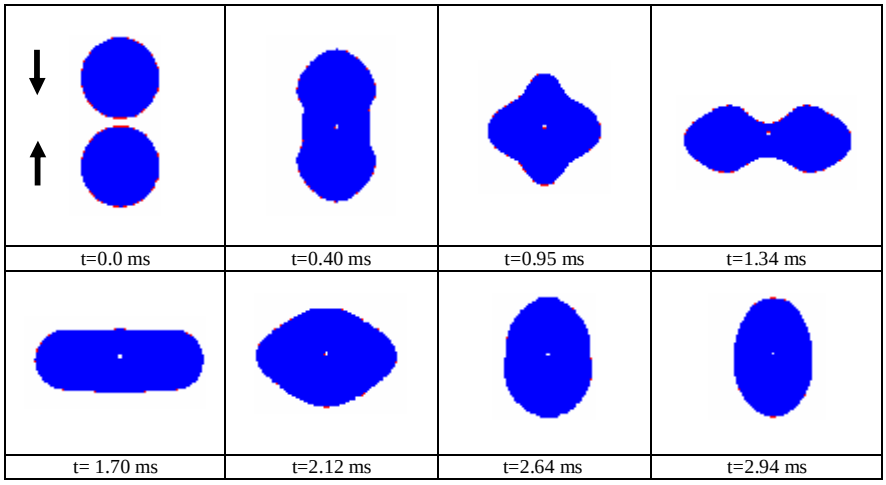

Figure 4: The effects of Re number on the coalescence collision of two drops: a) Re=240 and b) Re=480.

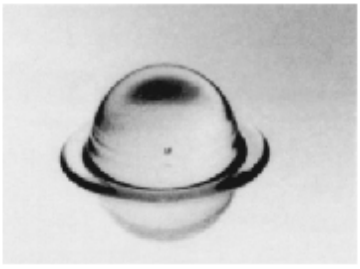

Figure 5: N-heptane impact on a stainless steel surface; air bubble is visible inside the drop [12].

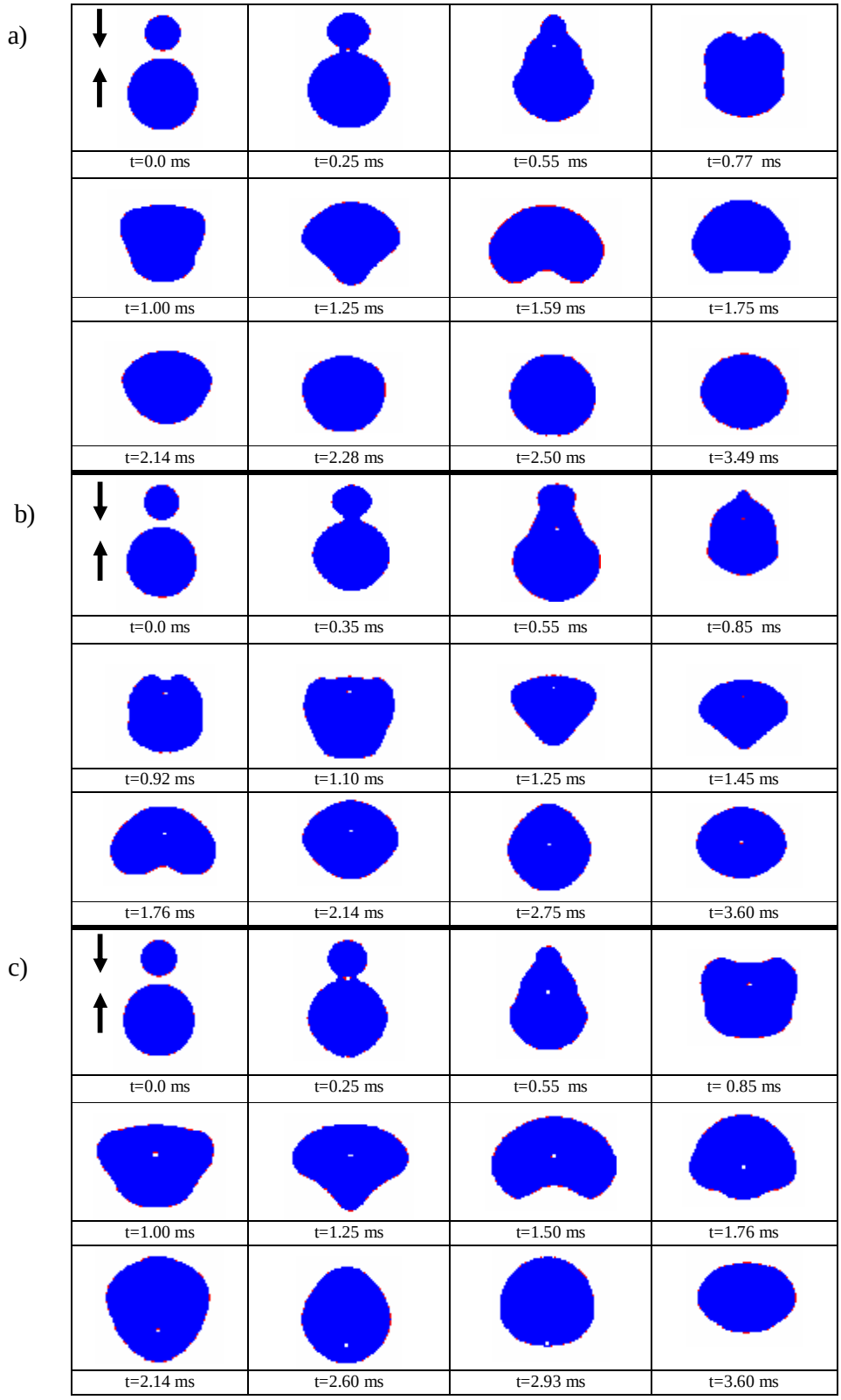

Figure 6: Time evolution of droplet deformation in an unequal drop collision with a size ratio of 0.5 a) V_u=0.30, V_l=0.0 b) V_u=0.15, V_l=0.15 and c) V_u=0.0, V_l=0.30 (V_u and V_l are velocities of the upper and lower drops towards each other, respectively).